Wavelet analysis of pulse tests in soil samples

Marcos Arroyo*

Summary

Measurement of elastic soil properties using transient dynamic movements (i.e. waves) is widespread both in the field and the laboratory. The wave model employed for the inversion problem must be simple, but representative of the measurement system. Data analysis and manipulation should facilitate the inversion procedure. Time and frequency domain approaches have both been employed for this purpose, but both face some limitations. Simultaneous time-frequency representations offer a tool to enhance data analysis. Wavelet transforms are a very successful method currently employed to obtain such representations. Here this method is applied to examine traces from laboratory pulse tests, both experimental and simulated.

Introduction

Geophysical field techniques are one of the classical tools in geotechnical characterization studies. Laboratory non-destructive testing is a relatively more recent addition but also a highly successful one [Santamarina *et al.*, 2001]. While the physical elements involved, sources, receivers, etc are different, there is a large conceptual common ground to both fields, for instance in their reliance on the detection of dynamic transient signals. These disturbances are generally small excursions from a stable state and, consequently, may be described approximately by linear theories.

The linear dynamic systems perspective is, therefore, a fertile approach from which to conceive test models. As Figure 1 illustrates with the example of laboratory pulse tests, the whole test can be conceived as a system relating input and output signals. This system may then be decomposed into several series-connected subsystems, representing, in the example, transducer operation and sample transmission. Note that further decomposition is possible, for instance separating various path-related effects such as transmission through the sample and end reflections. There is always a trade-off between the level of detail included in the model and its predictive abilities [Muir Wood, 1990].

Confrontation with measurements is how system models are validated or discarded. That confrontation usually requires some elaboration of the experimental data, of the model predictions or both. Dynamic signals are examined either in the time domain – for instance when looking for first arrivals of a wave in some time record of a motion - or in the frequency domain – for instance, while looking at the resonance frequency of a torsionally excited cylinder. The comparison may focus on some characteristic isolated elements of the response, as in the examples just mentioned, or may employ a greater portion of the recorded data – for instance, by trying to match the whole dispersion curve of the system, as done in the SASW. It is clear that the second technique is more ambitious, able to extract more information from the experimental signal and therefore more adequate when the system model is complex.

In this context it may be helpful to address the problem of system identification with newer, more powerful tools. One such tool is wavelet time-frequency analysis. This technique is well known in engineering mechanics [for instance, Kishimoto *et al.*, 1995; Le and Argoul, 2004] but, with a few exceptions [Haigh *et al.*, 2002; Kim and Park, 2002], has received less attention in the geotechnical field. In this paper the technique is briefly introduced and then exemplified with the search for multiple guided modes in laboratory pulse tests. The chosen application example requires some justification, and this is given first.

Laboratory pulse tests in soils

One important non destructive technique is laboratory pulse testing. Dynamic motions are generated and detected at various points in a soil sample (Fig. 2). Although other possibilities are available, piezoelectric transducers are generally employed for these tasks. The dynamic motion records are then usually interpreted to infer elastic soil properties. These elastic moduli are interesting for a variety of reasons. They may be directly plugged into soil elastodynamic models, common in earthquake engineering. They may be used as an upper stiffness limit in the simplified non-linear elasto-plastic mod-

* Departamento de Ingeniería del Terreno, UPC, Barcelona, Spain

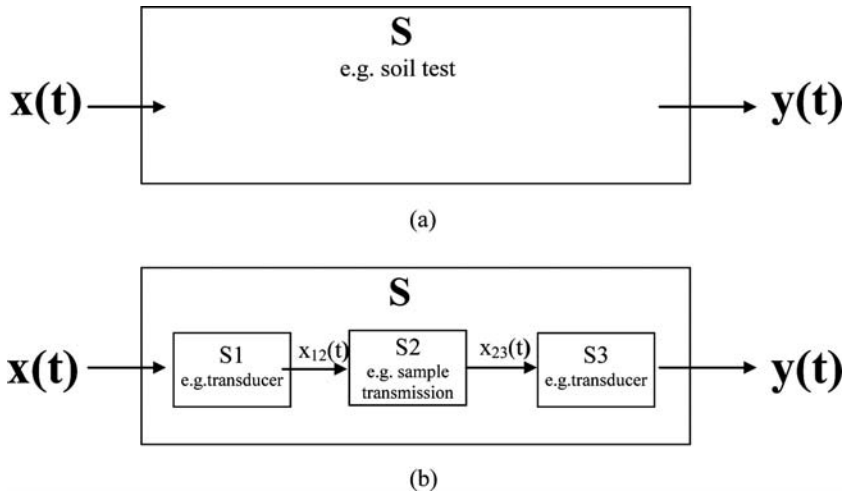

Fig. 1 – Dynamic systems for modelling seismic soil testing (a) without and (b) with internal sub-systems.
Fig. 1 – Sistemi dinamici per modellare prove sismiche sui terreni (a) senza e (b) con subsistemi interni.

els frequently employed to predict soil displacements around civil engineering structures. Finally, and since dynamic moduli are clearly dependent on soil state variables such as porosity, stress state or degree of structure, their variation may be employed to test more advanced soil behaviour models.

The interpretation of pulse tests to obtain elastic moduli is sometimes problematic. The dominant test model is that of plane wave propagation but, at least in some circumstances, it does result in large measurement uncertainty [ARROYO *et al.*, 2003a]. Parasitic effects due to test set-up geometry may hide the relevant material information. This is particularly worrying when the material information sought after is refined to include poroelastic effects [ARROYO, FERREIRA and SUKOLRAT, 2006] or anisotropic behaviour [ARROYO and MUIR WOOD, 2003].

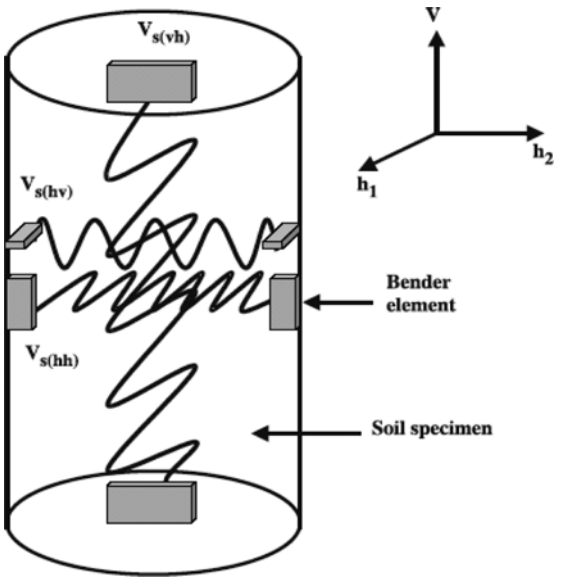

Fig. 2 – Example of a laboratory pulse test configuration (from PENNINGTON *et al.*, 1997).
Fig. 2 – Esempio di configurazione sperimentale per prove di trasmissione di onde elastiche in laboratorio [da PENNINGTON et al., *1997].*

Parasitic effects may be discounted using more complex test models. For instance, one type of parasitic effect, that due to the source near-field, may be dealt with by using the appropriate Stokes source model [ARROYO *et al.*, 2003b; LEE and SANTAMARINA, 2005]. A different type of parasitic effect is that due to sample boundary reflections. This effect is relevant for pulse propagation alongside the axis of cylindrical samples [ARROYO *et al.*, 2006], a common laboratory configuration, for instance, when testing in a triaxial apparatus.

A possible approach to discount or avoid this last problem makes use of guided wave theory [GRAFF, 1975]. The theory describes how elastic waves propagate alongside infinite cylinders. ARROYO *et al.*, [2002] argued that bender-element type transducers excite various flexural guide modes in the sample. Recently, HOLMAN and FINNO [2006] have presented some experimental results interpreted in the same framework. Their interpretation employs just the first flexural cylindrical mode. If the first flexural mode is the only one excited the modelling problem is simpler, because simplified beam theories, like that of Bernouilli-Euler or Timoshenko offer good approximations, at least on a restricted frequency range [THURSTON, 1992]. If higher order modes are excited the modelling problem is far more complex.

ARROYO *et al.*, [2002] analyzed results from numerical simulations of the problem to explore this issue, and found that various modes were seemingly being excited. However the numerical results were analyzed using a 2D FFT, a technique that requires several records of the same motion taken at differing locations – as exemplified by its SASW applications, FOTI [2000]. It will be very difficult to place

enough transducers on a sample to use the 2DFFT with experimental results and therefore the question about the number of modes excited in axial bender-based pulse tests remains open. As illustrated below, wavelet time frequency analysis may offer a way to solve this problem.

Wavelets and wavelet transforms

This section briefly summarises the basic concepts of wavelet theory useful for our application. A good introduction to the subject from the viewpoint of interest here might be found in ADDISON [2002], for more in-depth treatments see MALLAT [1999] or CARMONA *et al.* [1997].

Wavelet transform basics

Let us call f(t) the function or signal of interest. A continuous wavelet transform (CWT) of this function is obtained through

$$Wf(s,b) = \int_{-\infty}^{\infty} f(t)\Psi^*_{s,b}(t)\,dt \qquad s>0, b\in \mathbb{R} \tag{1}$$

Contrary to the Fourier transform, which is only dependent on one parameter, (the frequency), the wavelet transform of f(t) is bi-parametric, that is, it depends on the scale parameter, s, and the shift parameter, b. For each value of the pair (s,b), the symbol $\psi_{s,b}$ specifies a function belonging to a wavelet family, the * indicating complex conjugate. Wavelet families are obtained translating and scaling a function ψ, called mother wavelet,

$$\Psi_{s,b}(t) = \frac{1}{\sqrt{s}}\Psi\left(\frac{t-b}{s}\right) \tag{2}$$

For a fixed scale s the wavelet transform can be seen as a correlation with the scaled mother wavelet

$$Wf_s(b) = f(t)\otimes\frac{1}{\sqrt{s}}\Psi\left(\frac{t}{s}\right) \tag{3}$$

It is important to appreciate that scaling by a factor s has opposite effects on the time and frequency domain representations of a wavelet, since

$$\begin{gathered}\Psi(t) \xrightarrow{FT} \hat{\Psi}(\omega) \\ \frac{1}{\sqrt{s}}\Psi\left(\frac{t-b}{s}\right) \xrightarrow{FT} \sqrt{s}\,\hat{\Psi}(s\omega)\,e^{-i\omega b}\end{gathered} \tag{4}$$

When the scale s > 1 the mother wavelet is expanded in time domain and its spectrum contracted in frequency domain, the opposite effect resulting when s < 1.

Contrary to Fourier transforms, of which a large catalogue is available, explicit expressions for CWT are rare. One important exception is the harmonic exponential function, for which

$$\begin{aligned} f(t) &= e^{-i\omega_0 t} \\ Wf(s,b) &= \sqrt{s}\,\hat{\Psi}^*(s\omega_0)e^{-i\omega_0 b}\end{aligned} \tag{5}$$

Where the symbol $\hat{\Psi}$ represents the Fourier transform of the analysing wavelet.

The wavelet transform of a function *f*, *Wf*, is generally complex. Therefore we can distinguish between its modulus and its phase. The squared modulus of the transform is known as the scalogram of the function *f*

$$PWf(s,b) = |Wf(s,b)|^2 \tag{6}$$

A scale-normalised version of the scalogram is also commonly employed

$$SWf(s,b) = \frac{|Wf(s,b)|^2}{s} \tag{7}$$

ADDISON [2002] shows that the scalogram is proportional to the energy density in the time-frequency plane of the analysed signal.

The Gabor wavelet

The basic requirements for a mother wavelet are brief. The mother wavelet should have a mean value of zero and should have a fast decay. It is also useful, although not strictly necessary, for the mother wavelet to be of unit norm. The zero mean condition is equivalent to having a nil component at zero frequency. For analysis purposes it is also useful to employ what is known as analytic or progressive wavelets, that is wavelets such that their Fourier transform is real and vanishing for negative values.

A very commonly employed wavelet family [KISHIMOTO *et al.*, 1995; MALLAT, 1998; TYAS and WATSON, 2000; LANZA DI SCALEA *et al.*, 2004] is that generated by the Gabor wavelet. The time and frequency domain analytic expressions for the mother Gabor wavelet are:

$$\begin{aligned} \Psi(t) &= \frac{1}{(\pi\sigma^2)^{1/4}}e^{-\left(\frac{t^2}{2\sigma^2}\right)}e^{-i\eta t} \\ \hat{\Psi}(\omega) &= (4\pi\sigma^2)^{1/4}\,e^{-\frac{1}{2}(\omega-\eta)^2\sigma^2}\end{aligned} \tag{8}$$

The mother Gabor wavelet is an harmonic function of frequency η windowed by a gaussian window with mean zero and spread controlled by σ, the standard deviation. An example of this function is represented in Figure 3. The product of variance and central frequency has to be large enough (>5) to approximately abide with the zero mean condition.

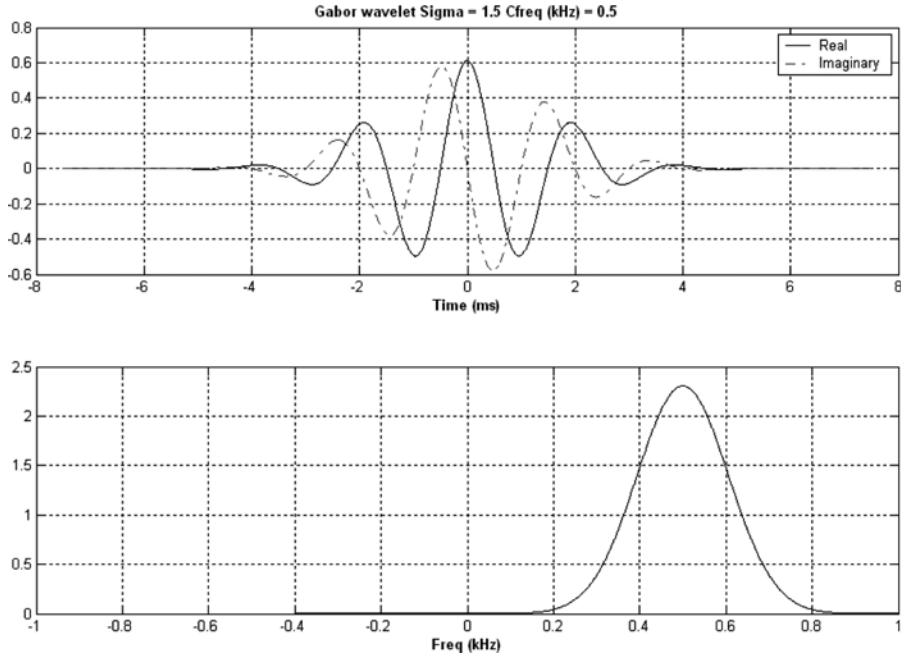

Fig. 3 – Gabor mother wavelet in time (above) and frequency domain (below).
Fig. 3 – Madre wavelet di Gabor nei domini di tempo (sopra) e frequenza (sotto).

Numerical evaluation

Here, the numerical evaluation of the CWT is based on the relation (3). For each scale the correlation between the analysed function and the scaled wavelet is computed as

$$Wf_s(b) = FFT^{-1}\left[\hat{f}(\omega)\sqrt{s}\,\hat{\Psi}^*(s\omega)\right] \qquad (9)$$

As usual for correlations [PRESS *et al.*, 1992] the operation is best done in the frequency domain using the FFT.

Time-frequency analysis using wavelets

Time-frequency atoms

It is well known that Fourier analysis gives the frequency content of a signal without any indication of when and if the frequency content of the signal varies within its record. Using a classical example, in Figure 4 we represent two different signals, both superposing the same short high frequency pulse and low frequency beat. The Fourier Transform of both

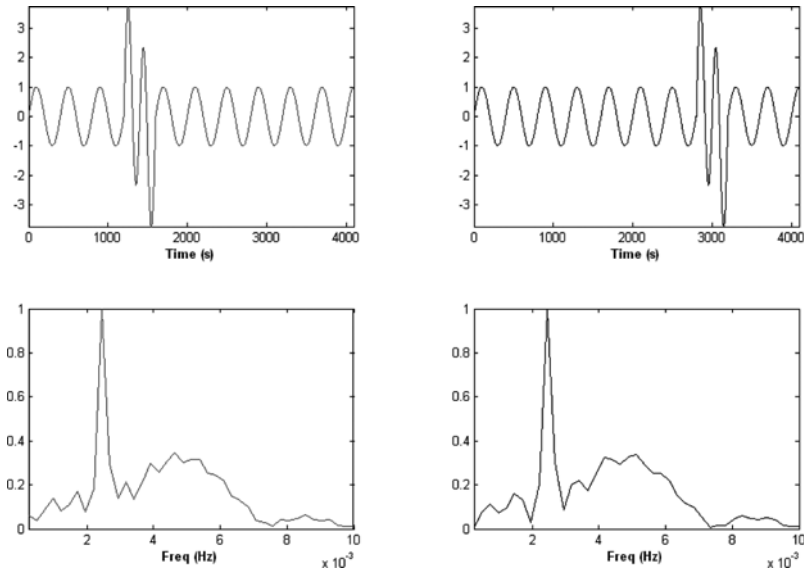

Fig. 4 – Two different transient signals (above) and their identical amplitude spectra (below).
Fig. 4 – Due segnali transitori distinti (sopra) e il loro spettro di frequenza identico (sotto).

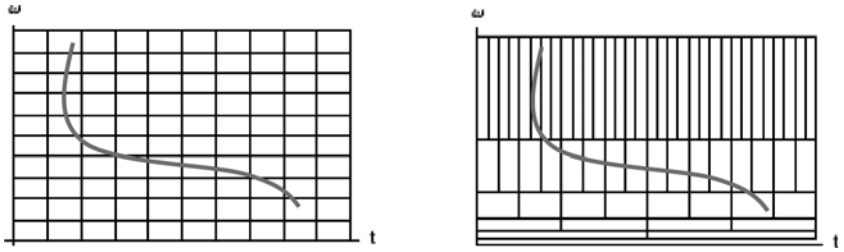

Fig. 5 – Schematic localization on the time-frequency plane of a base of windowed harmonics (left) and a wavelet base (right). Adapted from HARROP [2004].
Fig. 5 – Localizzazione schematica nel piano tempo-frequenza di una base di armoniche selezionate (a sinistra) e di una base wavelet (a destra) da HARROP [2004].

signals is shown below: there is no appreciable difference.

This situation is good enough when the process examined is stationary, or, in other words, if it may be assumed that the record examined will repeat itself forever (for instance, in the preceding example, because the phenomena underlying the high frequency pulse and the slow frequency beat are both cyclic). However, this assumption is not adequate for non-stationary processes. A good example may be a wave, essentially a transient process, that rises, oscillates for a while and finally decays.

Time-frequency analysis techniques were developed to overcome that limitation of Fourier analysis and deal with non-stationary processes. Linear time-frequency transforms correlate the signal with waveforms that are well concentrated in time and frequency, known as time-frequency atoms. These atoms will belong to a family, say $\{\phi_\gamma\}$, where γ are the parameter or parameters identifying each member of the family. For instance, in a wavelet family like (2) there are two parameters, the scale s and the shift b. Other families of time-frequency atoms frequently used are windowed harmonic functions.

Resolution in the time-frequency plane

Every time-frequency atom is localised in time and frequency. Depicting time and frequency as the orthogonal axes of a plane, the location of each atom may be characterised by several basic geometrical parameters. These are its centre coordinates in time and frequency, t_ϕ and ω_ϕ, and the equivalent radius, Δt_ϕ and $\Delta\omega_\phi$, also defined in time and frequency. These properties are obtained as follows

$$t_\phi=\frac{1}{\|\phi_\gamma\|^2}\int_{-\infty}^{\infty} t|\phi_\gamma(t)|^2 dt \qquad \omega_\phi=\frac{1}{\|\hat{\phi}_\gamma\|^2}\int_{-\infty}^{\infty}\omega|\hat{\phi}_\gamma(\omega)|^2 d\omega$$
$$\Delta t_\phi=\frac{1}{\|\phi_\gamma\|^2}\sqrt{\int_{-\infty}^{\infty}(t-t_0)^2|\phi_\gamma(t)|^2 dt} \qquad \Delta\omega_\phi=\frac{1}{\|\hat{\phi}_\gamma\|}\sqrt{\int_{-\infty}^{\infty}(\omega-\omega_0)^2|\hat{\phi}_\gamma\omega)|^2 d\omega} \tag{10}$$

The centre and radius definition just given are exactly like those of the mean and standard deviation of a statistical distribution. It is therefore also appropriate to conceive of the radius of an atom as a measure of its resolution in the time-frequency plane. An important result in this respect is the so-called "Heisenberg uncertainty principle" [MALLAT, 1999]. It states simply that no function has perfect localization in time and frequency, and that there is a lower bound to the product of time and frequency uncertainty[1]

$$\Delta t_\phi \Delta\omega_\phi \geq \frac{1}{2} \tag{11}$$

Table I summarises the basic time-frequency geometric properties of a generic mother wavelet, ψ, and its translated and scaled daughters, $\psi_{s,b}$. We have also included in the table the results for the Gabor wavelet [SIMONOVSKI and BOLTEZAR, 2003].

Tab. I – Characteristic values of a generic mother wavelet, of a generic wavelet and of the Gabor mother wavelet.
Tab. I – Valori caratteristici della madre di una wavelet generica, di una wavelet generica e della madre di una wavelet di Gabor.

	t_ϕ	ω_ϕ	Δt_ϕ	$\Delta\omega_\phi$
Ψ	t_Ψ	ω_Ψ	Δt_Ψ	$\Delta\omega_\Psi$
$\Psi_{s,b}$	$st_\Psi+b$	$\frac{\omega_\Psi}{s}$	$s\Delta t_\Psi$	$\frac{\Delta\omega_\Psi}{s}$
Gabor Ψ	0	η	$\frac{\sigma}{\sqrt{2}}$	$\frac{1}{\sqrt{2}\sigma}$

The increasing spread of a daughter wavelet on the time axis is exactly compensated by its reduced spread on the frequency axes. A wavelet decomposition has very good time resolution at small scales and very good frequency resolution at higher scales. As we will explain below, scale is inversely proportional to frequency, therefore time resolution is enhanced at high frequency. Since high-frequency events are sharply localised in most signals of interest, there lies the attractiveness of the wavelet technique. This is illustrated in Figure 5 where the time-frequency localization properties of a wavelet family are compared with those of a windowed harmonic family.

[1] It is in this context where Fourier analysis can be seen as a particular case of wavelet analysis. The Fourier atoms are perfectly localised in frequency ($\Delta\omega_\phi = 0$) but not localised at all in time ($\Delta t_\phi = \infty$).

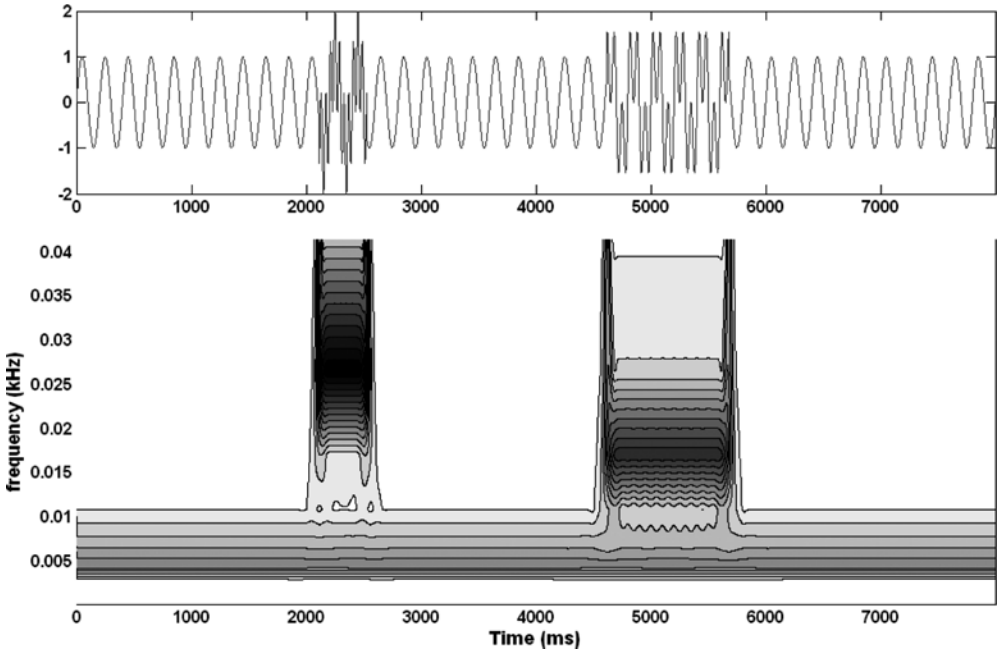

Fig. 6 – Normalised scalogram of an harmonic signal of basic frequency f = 5 Hz with two superimposed signals of frequency 5*f (at time 2.11 to 2.53 s) and 3*f (at time 4.62 to 5.68). Gabor wavelet with σ = 1 and η = 5.
Fig. 6 – Scalogramma normalizzato di un segnale armonico di bassa frequenza (f = 5 Hz) con due segnali sovrapposti di frequenza 5f (fra i tempi 2.11 a 2.53) e 3f (fra i tempi 4.62 a 5.68). Wavelet di Gabor con σ = 1 e η = 5.

Scale and frequency relationship

It is necessary to establish a relation between scale and frequency to obtain a time-frequency representation of a signal from its CWT. Rigorously, this relation is established only locally, at certain points of the wavelet transform. A typical choice is that of the transform ridges, or normalised scalogram maxima [ADDISON, 2002]. On the ridges we have

$$\frac{\partial SWf(s,b)}{\partial s}=0 \qquad (12)$$

This condition is combined with the expression of the WT of the harmonic function, (5), to obtain a specific frequency-scale relation. For the Gabor wavelet, this leads to

$$SW_{Gabor}(e^{i\omega t})=(4\pi)^{1/2}\sigma e^{-(\omega s-\eta)^2} \qquad (13)$$

Finding the maxima of this expression the following frequency-scale relation is obtained

$$\omega=\frac{\eta}{s_R} \qquad (14)$$

where s_R indicates the scale on the ridge.

Time-frequency wavelet maps

The scale-frequency relation above might then be employed to interpret the normalised scalogram of a signal as a time-frequency map. The scalogram offers a way to continuously identify the varying frequency content of the signal. In fact, the identification given by the frequency axis only holds true at the maxima of the figure, and these maxima are somewhat blurred due to the resolution limitations inherent in the wavelet choice. Notwithstanding these limitations, the technique is able to separate superposed signals in enough circumstances to make it worthwile. An example of application is given in Figure 6, in which several short-frequency pulses are superposed on a continuous beat. Next we will see how it might be applied in wave propagation problems.

Time-frequency wave propagation signatures

Wave motion and transfer functions

Natural motions are often described as harmonic waves, whose general expression, for any motion component, u, is given by

$$u(\mathbf{x},t)=a(\mathbf{x})\cos\left[\Theta(\mathbf{x},t)\right]=\mathrm{Re}\left\{a(\mathbf{x})\exp\left[\Theta(\mathbf{x},t)\right]\right\} \qquad (15)$$

Where a is the movement amplitude, and Θ is the phase function. Surfaces of constant phase are known as wavefronts; the phase time derivative, ω, is known as frequency, and its spatial gradient as the wavevector.

In many circumstances there is a privileged spatial direction, say z, orthogonal to the wavefront, along which the periodicity of the motion is revealed.

$$u(\mathbf{x},t,\omega)=a(x_i)e^{-i(\overline{k}z-\omega t)}\; x_i\neq z \qquad \overline{k}=k+ik_i \tag{16}$$

Where k is the wavenumber, now the only non-zero component of a wavevector directed along z. Such wave motions have to abide with material and geometric restrictions (i.e. with constitutive relations and boundary conditions) to be acceptable solutions of a mechanical problem. These extra restrictions often translate into links between wavenumber, frequency and amplitude. The link between wavenumber and frequency is known as the dispersion relationship.

$$u(\mathbf{x},t,\omega)=a(x_i,\omega)e^{-i(\overline{k}(\omega)z-\omega t)} \tag{17}$$

A general time-dependent motion can be obtained if we use frequency as a parameter and sum for all possible frequencies

$$u(\mathbf{x},t)=\frac{1}{2\pi}\int_{-\infty}^{\infty}a(x_i,\omega)e^{-i(\overline{k}(\omega)z-\omega t)}\,d\omega \tag{18}$$

If we fix now the non-propagation coordinates, x_i, and consider the inverse Fourier transform definition, the preceding expression can be seen as a convolution product of two time-dependent functions

$$u(z,t)=\frac{1}{2\pi}\int_{-\infty}^{\infty}a(\omega)e^{-i(\overline{k}(\omega)z)}e^{i\omega t}d\omega=u_0(t)*s(z,t) \tag{19}$$

Using now the linear system language, in the function $s(z,t)$, we have a z-dependent characteristic system response function, and the corresponding system transfer function, $S(z,\omega)$, is given by

$$S(z,\omega)=e^{-i\overline{k}(\omega)z} \tag{20}$$

The input function, $u_0(t)$, is simply the motion at $z=0$, as can be seen substituting that value in (19) above.

Therefore, the dispersion relation gives the transfer function between the wave motion recorded at the z-coordinate origin and that recorded at any propagation distance z. The dispersion relation of a wave motion identifies the elastodynamic system under study; and vice versa, measurement of the dispersion relation offers an appropriate experimental means of system identification.

Phase velocity, group velocity and group delay

The wavefront moves and the normal to the wavefront has an instantaneous velocity known as phase velocity. This is generally a vector, whose modulus, v, is known also as phase velocity. Differentiating the phase function shows that wavenumber, phase velocity and frequency are related through

$$vk=\omega \tag{21}$$

Another quantity with velocity dimensions is called group velocity and defined as

$$v_g=\frac{\Delta\omega}{\Delta k} \tag{22}$$

There are two important related aspects here. First, group velocity is also the velocity at which energy is propagated by the wave [see UDIAS, 1999, 3.4]. Second, in general signal processing terms [e.g. OPPENHEIM and SCHAFFER, 1975] the group delay of a transfer function, $\tau(\omega)$, is defined as minus the frequency derivative of its phase. For a dispersive wave this makes perfect sense, since we have

$$\tau(\omega)=-\frac{\Delta\Theta}{\Delta\omega}=\frac{\Delta k}{\Delta\omega}z=\frac{z}{v_g}=t_g \tag{23}$$

It is clear then that in a dispersive wave the group delay is, literally, the travel time of any given frequency. Also, the group delay function, $\tau(\omega)$ can be obtained as the derivative of a dispersion relation $k(\omega)$.

Group delay and CWT

Since the CWT maps the energy of a signal and energy in waves travels at the group velocity, the CWT may be employed to obtain wave group velocity. If we have a system where a wave propagates like (19), the CWT of the output signal would give its time-frequency map, allowing us to obtain, at its ridges, a time-frequency relationship, $t(\omega)_{\text{output}}$. Clearly, this may be decomposed as

$$t(\omega)_{output}=t(\omega)_{input}+\tau(\omega) \tag{24}$$

That is, the time at which each frequency appears at the output is the sum of the time at which it was input into the system plus the group delay due to the wave transmission. The first member of the sum, $t(\omega)_{\text{input}}$, might be obtained independently by means of the CWT of the input signal.

Obtaining the dispersion curve

The procedure just explained can be employed to obtain the group delay corresponding to any transfer function in a pulse transmission test. Integration of the group delay curve will give the dispersion relation characterising the system. Even better,

knowing the measurement location z, the group velocity curve of the wave would be directly obtained.

Two numerical experiments, inspired by those in WOOH and VEROY [2001a], will now illustrate the procedure. We specify a dispersion relation, use it to construct a wave transfer function and propagate a pulse through the system thus characterised. Then we do a CWT of both input and output signals and plot them together. The dispersion relations specified are the following, expressed first with the standard wavenumber-frequency form and then as group velocity vs frequency

$$\begin{aligned} k^a(\omega) &= \frac{\omega}{v} \quad v_g^a = v \\ k^b(\omega) &= \frac{\sqrt{\omega_0 \omega}}{c} \quad v_g^b = 2c\sqrt{\frac{\omega}{\omega_0}} \end{aligned} \tag{25}$$

The first relation, k^a, is linear and therefore corresponds to the case of non-dispersive propagation, for instance that of plane bulk shear wave, with v the bulk shear wave velocity. The second is a typical example [DOYLE, 1997, Chapter 1] of a properly dispersive case, with ω_0 a parameter of frequency dimension and c a parameter of velocity dimension. The input signal in both cases is a half-sine pulse of apparent frequency f_{ap}=10 Hz.

Figure 7 illustrates the non-dispersive case, for v = 1 km/s and a propagating distance of 3 km. After exactly 3 seconds the input signal is exactly recorded at the output. The scalogram of this output is an exact shifted copy of the input, with energy almost equally distributed in the 5 to 50 Hz band of the graph.

Figure 8 corresponds to the dispersive case, with ω_0 = 1cps and c = 50 m/s. The dispersion relation implies a group velocity that increases indefinitely and monotonically with frequency (such a property is a physical impossibility, but the relation may be a good approximation to physical systems in a restricted frequency range). Higher frequencies, therefore, arrive earlier than lower frequencies. This is already visible on the time trace of the output, but is made patent on the scalogram. The dotted line on the scalogram indicates the arrival time according to the theoretical dispersion relationship. As expected, this theoretical arrival time coincides reasonably well with the line of maxima of the scalogram.

Multimodal transmission and CWT

In some systems there might be several active modes of wave transmission acting simultaneously. Each mode will be characterised by a particular dispersion equation and transfer function like that in (20). Since the wavelet transform is linear and the contribution of each mode to the transmission is additive, it is possible to apply the procedure explained above to the sum. In the CWT of the composed signal each mode would leave its specific trace on the scalogram. An example of this follows in the next section.

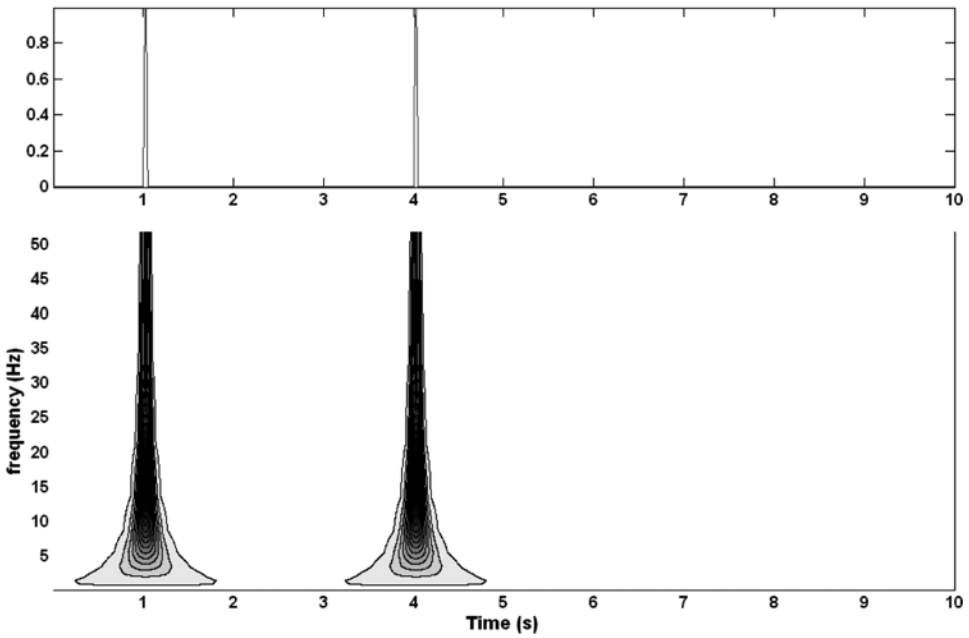

Fig. 7 – Non-dispersive propagation of a pulse signal (above) and normalised scalogram (below). Gabor wavelet with σ = 1 and η = 5.

Fig. 7 – Propagazione non-dispersiva di un segnale (sopra) e il suo scalogramma normalizzato (sotto). Wavelet di Gabor con σ=1 e

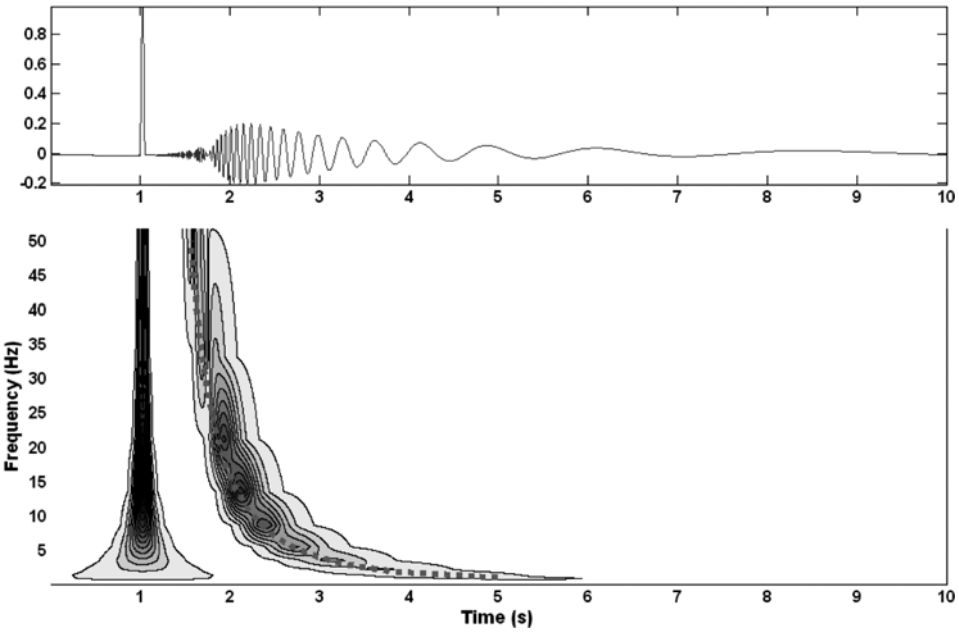

Fig. 8 – Dispersive propagation of a pulse (above) and normalised scalogram (below). Gabor wavelet with $\sigma = 1$ and $\eta = 5$.
Fig. 8 – Propagazione dispersiva di un segnale (sopra) e il suo scalogramma normalizzato (sotto). Wavelet di Gabor con $\sigma = 1$ e $\eta = 5$.

Guided waves and pulse tests

Guided cylindrical waves

The term waveguide is used to describe situations where a wave is propagated in structures, like rods, plates or geological strata, whose shape directs the motion along a favoured dimension of the structure [GRAFF, 1975]. Waveguide effects in rods are described for instance in THURSTON [1992]. Adopting a system of cylindrical coordinates, guided waves in this case can be synthetically expressed as motions given by

$$\mathbf{u}(r,\theta,z,t) = \mathbf{A}(r,\theta)\cos[\omega t - kz] \qquad (26)$$

The first term in (26) describes the shape of the movement within the circular section of the cylinder and the second term how this shape propagates along the cylinder. For infinite rods, any forced motion may be expressed as a linear combination of its modes, i.e. solutions of the elastodynamic homogeneous problem. Each of these modes, M_{nm}, is characterised by its modal shape A_{nm} and modal dispersion curve $k_{nm}(\omega)$.

There are three families of cylindrical modes: torsional, longitudinal and flexural. Usual bender element implementations have them located axially on cylindrical samples. Some consideration of modal shapes [ARROYO, 2001] shows that flexural modes would be those most likely to be excited by bender action. Computing the modal characteristics – dispersion curve and modal shape – for a bar of known radius and material properties is numerically involved. Using "Disperse" [PAVLAKOVIC and LOWE, 2000] we have evaluated them for a bar tailored to simulate an unconfined soil cylinder ($r = 5$ cm; $v_s = 120$ m/s; $\nu = 0.1$). Figure 9 shows a selection of the resulting modal dispersion curves – plotted as group velocity vs frequency – in a frequency range typical of soil pulse tests.

CWT of simulated signals

After generating the dispersion curves with "Disperse" it is also possible to use them to numerically propagate signals, using transfer functions constructed as in (20). We have done so to propa-

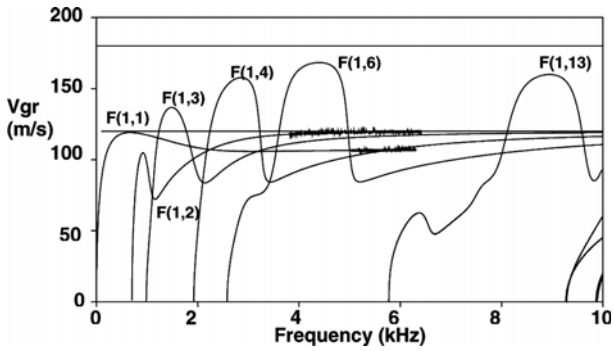

Fig. 9 – Group velocity curves of various flexural modes of an elastic cylinder of $r = 5$ cm; $v_s = 120$ m/s; $\nu = 0.1$.
Fig. 9 – Curve di velocità di gruppo corrispondenti a diversi modi flessurali di un cilindro elastico con $r = 5$ cm; $v_s = 120$ m/s; $\nu = 0.1$.

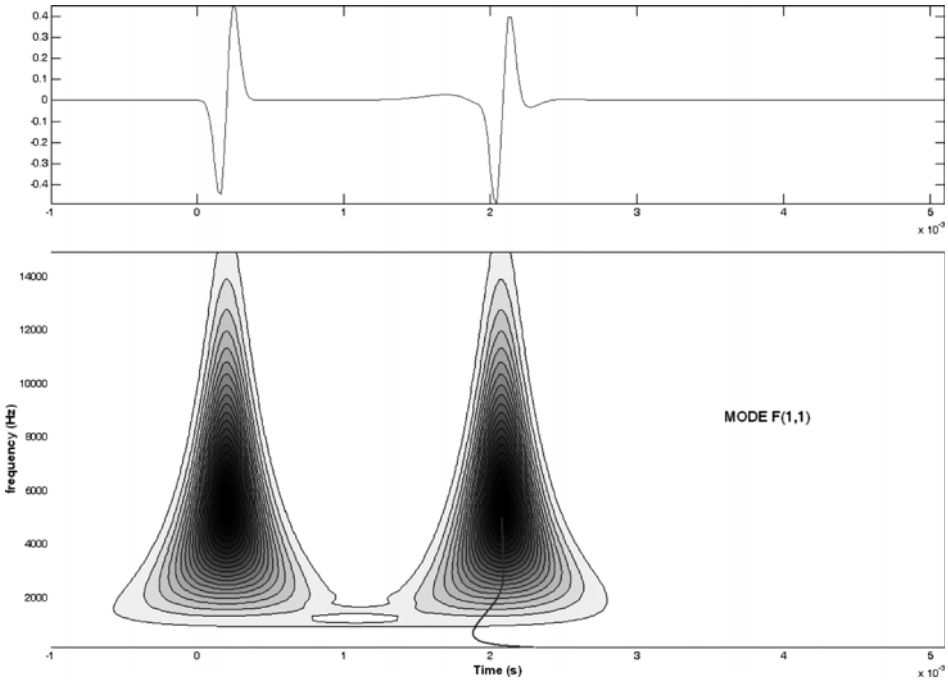

Fig. 10 – Wavelet analysis of a signal numerically propagated in a cylinder. Cylinder properties $V_s = 120$ m/s $\nu = 0.1$, radio 5 cm. Gabor wavelet with $\sigma = 1$ and $\eta = 5$.
Fig. 10 – Analisi wavelet di un segnale che si propaga numericamente in un cilindro. Proprietà dal cilindro: $V_s = 120$ m/s, $\nu = 0.1$, radio 5 cm. Wavelet di Gabor con $\sigma = 1$ e $\eta = 5$.

gate a single-cycle gaussian-windowed 2.5 kHz sinus. The propagated signal is then analysed using the CWT with a Gabor wavelet.

In a first exercise we have used as propagator only the first flexural mode. The propagation distance is 200 mm. In Figure 10 the scalogram of the signal thus produced is presented. Superposed onto the scalogram a group delay curve, identified as F(1,1), has been drawn. The input signal has most of its energy on the non-dispersive frequency range of the mode and therefore it suffers from very little distortion. The group delay curve overlaps well with the scalogram ridge. Note that here the input delay has been selected as a frequency independent 0.2 ms.

In a second exercise the same input and propagation distance are employed, but now two different flexural modes propagate the signal. The output is the direct sum of these two modes, with equal amplitude at each frequency. The input signal is now more clearly distorted by the transmission. In Figure 11 this signal and the corresponding scalogram are presented. It appears that, at least in the mid frequency range, the scalogram has two distinct elevations, separated by a valley. The location of those elevations seems to coincide reasonably well with that of the different mode arrivals predicted by the group delay curves.

Experimental signals

A result taken from a published database [ARROYO *et al.*, 2003a] will serve to illustrate the potential of the method with experimental signals. The tests were made on a laboratory bench, with bender elements located at the axial ends of a Gault clay cylinder of 98 mm diameter. The input signal is a 6 kHz square pulse traversing a distance of 121 mm. The signal and its scalogram are shown in Figure 12. At the time scale of the figure the input signal is short enough for all its frequency content to appear almost simultaneously. On the output at least two different elevations are clearly visible. They seem to indicate that in this test the energy input to the sample is travelling using at least two different propagation modes.

Discussion

To avoid ambiguities in group delay determination, the CWT based method just shown is best applied with a very broadband excitation, one in which all the frequencies enter the sample in a very short time. When testing metals, this is physically implemented using a laser source. Impact sources have also been employed. Bender elements and other piezoelectric sources employed in the soils laboratory are resonant sources, and do therefore complicate broadband testing.

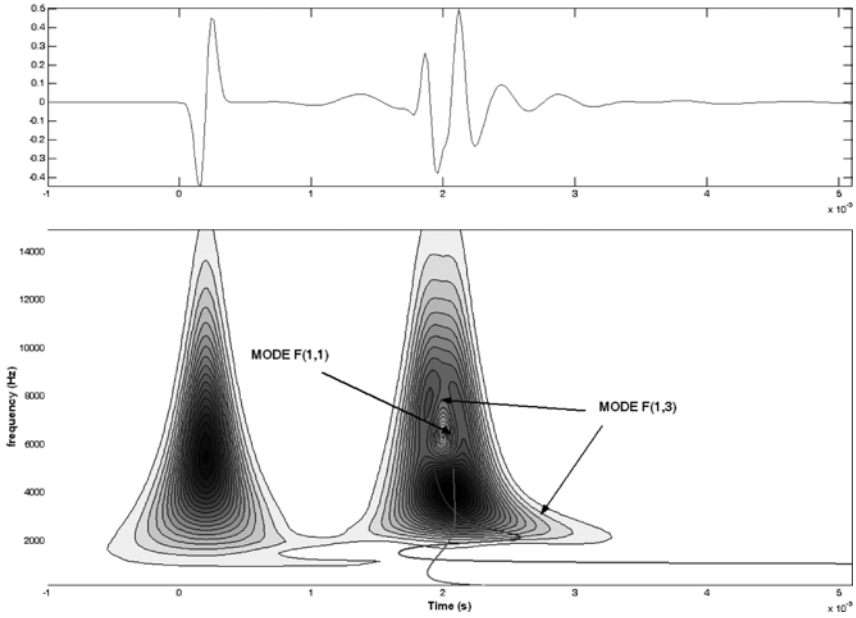

Fig. 11 – Wavelet analysis of a bi-modal signal numerically propagated in a cylinder. Cylinder and signal properties as above. Gabor wavelet with $\sigma = 1$ and $\eta = 5$.
Fig. 11 – Analisi wavelet di un segnale bimodale propagato numericamente in un cilindro. Proprietà dal segnale e dal cilindro come sopra. Wavelet di Gabor con $\sigma = 1$ e $\eta = 5$.

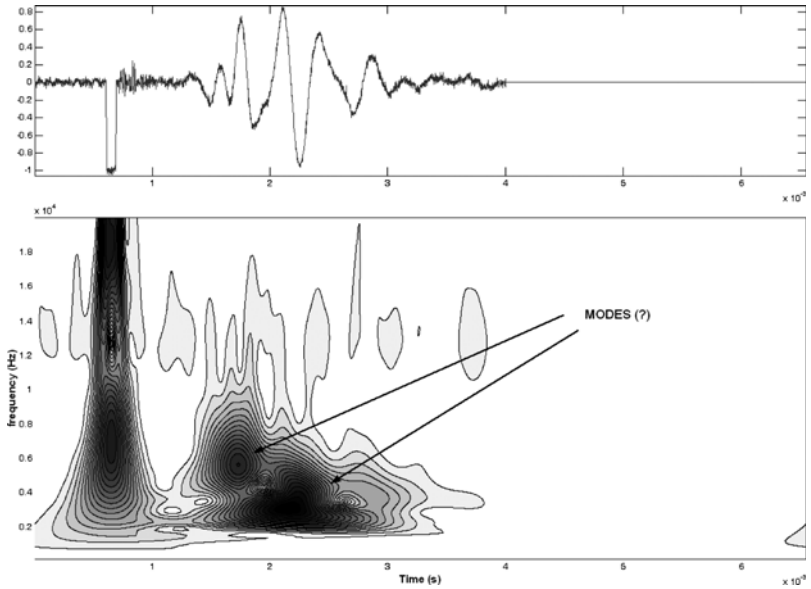

Fig. 12 – Scalogram of an input pulse signal and its response in a through transmission test in reconstituted Gault clay. 121 mm transmission distance, 6 kHz apparent pulse frequency. Gabor wavelet with $\sigma = 1$ and $\eta = 5$.
Fig. 12 – Scalogramma di un segnale input e la sua risposta in una prova di trasmissione di onde elastiche su argilla Gault ricostituita. Distanza di trasmissione 121 mm. Frequenza apparente dell'input 6 kHz. Wavelet di Gabor con $\sigma = 1$ e $\eta = 5$.

No attempt has been made above to use a proper modal weighting scheme to obtain a simulated signal to compare with the experimental signal. This is a task that is beyond the abilities of "Disperse" and that perhaps would require a different, more specific, approach [LI and BERTHELOT, 2000].

There are several other possible geotechnical applications of the CWT technique discussed in this paper. Two other cases where multimodal propagation is an issue in a geotechnical context are SASW testing in inverted profiles [FOTI, 2000] or dynamic inspection of piles [FINNO and CHAO, 2005]. The difficulties here signalled for the bender transmission case (lack of a predictive model and relative inadequacy of the input signals) are not present in these cases.

The CWT method has many other aspects worth discussing, but they are beyond the scope of this paper. For instance, when a proper modal model is available, the comparison of experimental and theoretical curves will be enhanced by explicitly extracting the ridges from the CWT scalogram. There are a number of techniques available for that purpose [CARMONA *et al.*, 1997]. It is also clear that not all the mother wavelets are equally suitable to separate modes and that no attempt has been made here to optimize the parameters of the Gabor wavelet in this respect [KIM and KIM, 2001] or even to compare different families [LE and ARGOUL, 2005].

Conclusion

Wavelet analysis is a practical and powerful tool to explore the time-frequency features of dynamic signals. Such features are useful for inverse analysis in complicated cases, for instance, those involving multimode propagation. For the case of pulse tests in soil samples the CWT method has been shown here to offer some evidence of multimodal propagation.

Acknowledgements

The research described in this paper started while the author was working at the Department of Civil and Environmental Engineering, University College London, funded by EPRSC Grant GR/T12187/01.

References

ADDISON P.S. (2002) – *The illustrated wavelet transform handbook*. IOP Publishing, Bristol.

ARROYO M., MUIR WOOD D., GREENING P., RIO J., MEDINA L. (2006) – *Effects of sample size on bender-based axial G0 measurements*. Géotechnique, 56, 1, pp. 39-52.

ARROYO M., FERREIRA C., SUKOLRAT J. (2006) – *Dynamic measurements and porosity in saturated triaxial specimens.* Soil Stress-Strain Behavior: Measurement, Modeling and Analysis, Geotechnical Symposium in Roma, March 16-17, 2006, (Eds. Ling *et al.),* Springer (to appear).

ARROYO M., GREENING P., MUIR WOOD D. (2003a) – *An estimate of uncertainty in current pulse test practice.* Rivista Italiana di Geotecnica, 37, 1, pp. 17-35.

ARROYO M., MUIR WOOD D. (2003) – *Simplifications related to dynamic measurement of anisotropic G_0.* Lyon'03 International symposium on deformation behaviour of geomaterials, (Eds. Di Benedetto *et al.*), Balkema, Rotterdam, pp. 1233-1239.

ARROYO M., MUIR WOOD D., GREENING P. (2003b) – *Source near-field effects and pulse tests in soil samples*. Géotechnique, 53, 3, pp. 337-345.

ARROYO M., MEDINA L., MUIR-WOOD D. (2002) – *Scale effects in bender-based pulse tests*. Numerical Methods in Geomechanics, NUMOG VIII, (Eds. Pande and Pietrusckzak) Balkema, pp. 589-595.

ARROYO M. (2001) – *Pulse tests in soil samples*. PhD Thesis, University of Bristol.

CARMONA R., HWANG W.L., TORRESANI B. (1998) – *Practical time-frequency analysis*. Academic Press.

DOYLE J.F. (1997) – *Wave propagation in structures*. 2nd Ed, Springer, New York.

FINNO R.J., CHAO H. (2005) – *Guided waves in embedded concrete piles.* ASCE J. of Geotechnical and Geoenvironmental Eng., 131, 1, pp. 11-19.

FOTI S. (2000) – *Multistation methods for geotechnical characterisation using surface waves*. PhD, Politecnico di Torino.

GRAFF K.F. (1975) – *Wave motion in elastic solids*. Clarendon Press, Oxford.

HAIGH S.K., TEYMUR B., MADABUSHI S.P.G., NEWLAND D.E. (2002) – *Applications of wavelet analysis to the investigation of the dynamic behaviour of geotechnical structures*. Soil Dynamics and Earthquake Engineering, 22, pp. 995-1005.

HARROP J.D. (2004) – *Structural properties of amorphous materials*, PhD Thesis, University of Cambridge.

HOLMAN T.P., FINNO R.J. (2006) – *Maximum shear modulus and incrementally nonlinear soils*. XVI ICSMGE, Osaka, vol. I, pp. 383-386.

LEE J.-S., SANTAMARINA J.C. (2005) – *Bender elements: performance and signal interpretation*. ASCE Journal of Geotechnical and Geoenvironmental Engineering, 131, 9, pp. 1063-1070.

KIM D.-S., PARK H.-C. (2002) – *Determination of dispersive velocities for SASW method using harmonic wavelet transform*. Soil dynamics and Earthquake Engineering, 22, pp. 675-684.

KIM Y.Y., KIM E.H. (2001) – *Effectiveness of the continuous wavelet transform in the analysis of some dispersive elastic waves*. Journal of the Acoustic Society of America, 110(1), pp. 86-94.

KISHIMOTO K., INOUE H., HAMADA M., SHIBUYA T. (1995) – *Time frequency analysis of dispersive waves by means of wavelet transform*. ASME Journal of Applied Mechanics, 62, pp. 841-846.

LANZA DI SCALEA F., MCNAMARA J. (2004) – *Measuring high-frequency wave propagation in railroad tracks by joint time-frequency analysis.* Journal of Sound and Vibration, 273, pp. 637-651.

LE T.P., ARGOUL P. (2004) – *Continuous wavelet transform for modal identification using free decay response*. Journal of Sound and Vibration, 277, pp. 73-100.

LI Z., BERTHELOT Y.H. (2000) – *Propagation of transient ultrasound in thick annular waveguides: modeling, experiments and application*. NDT&E International, 33, pp. 225-232.

LU L., ZHANG B. (2004) – *Analysis of dispersion curves of Rayleigh waves in the frequency-wavenumber domain*. Canadian Geotechnical Journal, 41, pp. 583-598.

MALLAT S. (1999) – *A wavelet tour of signal processing*. 2nd Ed, Academic Press, London.

MUIR WOOD D. (1990) – *Soil behaviour and critical state soil mechanics*. CUP.

OPPENHEIM A.V., SCHAFER R.W. (1975) – *Digital signal processing*. Prentice Hall.

PENNINGTON D.S., NASH D.F.T., LINGS M.L. (1997) – *Anisotropy of go shear stiffness in Gault clay*. Géotechnique, 47, n. 3, pp. 391-398.

PRESS W.H., TEUKOLSKY S.A., VETTERLING W.T., FLANNERY B.P. (1992) – *Numerical recipes in Fortran 77. The art of scientific computing*. 2nd Ed CUP.

SANTAMARINA J.C., KLEIN K.A., FAM M.A. (2001) – *Soils and Waves: Particulate Materials Behavior, Characterization and Process Monitoring*. John Wiley & Sons, New York.

SIMONOVSKI I., BOLTEZAR M. (2003) – *The norms and variances of the Gabor, Morlet and general harmonic wavelet functions*. Journal of Sound and Vibration, 264, pp. 545-557.

THURSTON R.N. (1992) – *Elastic waves in rods and optical fibers*. J. Sound Vib. 159(3), pp. 441-467.

TYAS A., WATSON A.J. (2000) – *A study of the effect of spatial variation of load in the pressure bar*. Meas. Sci. Technol. 11, pp. 1539-1551.

UDÍAS A. (1999) – *Principles of seismology*. Cambridge University Press.

WOOH S.C., VEROY K. (2001) – *Spectro temporal analysis of guided-wave pulse-echo signals: Part 1. Dispersive systems*. Experimental Mechanics. 41(4), pp. 324-331.

Analisi wavelet di prove con trasmissione di onde elastiche in campioni di terreno

Sommario

La misura delle proprietà elastiche dei terreni per mezzo di movimenti transitori (onde) è molto comune tanto in laboratorio come in situ. Il modello elastodinamico adoperato per l'analisi inversa deve essere semplice, ma allo stesso tempo rappresentativo del sistema di misura. L'analisi dei dati sperimentali e la loro manipolazione deve facilitare il procedimento d'inversione. Per questo si utilizzano, di solito, rappresentazioni di dati sia nel dominio frequenziale sia in quello temporale, ma entrambe hanno alcune limitazioni. Le rappresentazioni simultanee tempo-frequenza offrono un mezzo per migliorare l'analisi dei dati sperimentali. Le trasformate wavelet sono un metodo efficiente per ottenere queste rappresentazioni. Questo metodo viene applicato in questa occasione per analizzare le tracce ottenute nelle prove, simulate e sperimentali, di trasmissione d'onde in campioni di terreno.